The Journal of Neuroscience, July 1993, 13(7): 3051–3063

Differential Immunohistochemical Localization of Inositol 1,4,5-Trisphosphate- and Ryanodine-sensitive Ca^{2+} Release Channels in Rat Brain

Alan H. Sharp,[1] Peter S. McPherson,[5] Ted M. Dawson,[1,2] Chiye Aoki,[6] Kevin P. Campbell,[5] and Solomon H. Snyder[1,2,3,4]

Departments of [1]Neuroscience, [2]Neurology, [3]Pharmacology and Molecular Sciences, and [4]Psychiatry and Behavioral Sciences, Johns Hopkins University School of Medicine, Baltimore, Maryland 21205, [5]Howard Hughes Medical Institute, Department of Physiology and Biophysics, Program in Neuroscience, University of Iowa, College of Medicine, Iowa City, Iowa 52242, and [6]Center for Neural Science and Biology Department, New York University, New York, New York 10003

Ca^{2+} release from inositol 1,4,5-trisphosphate (IP_3)-sensitive and ryanodine-sensitive intracellular Ca^{2+} stores is mediated by distinct proteins identified as IP_3 receptors (IP_3R) and ryanodine receptors (RyR), respectively. We have compared the immunohistochemical localizations of IP_3R and RyR in the brain at the light and electron microscopic levels and have also evaluated the distribution of the major brain intracellular Ca^{2+}-pumping ATPase.

IP_3R and RyR occur in overlapping populations of neurons in widespread areas of the brain, but labeling is distinct in a number of areas. For example, IP_3R is enriched in cerebellar Purkinje cells and hippocampal CA1 pyramidal cells, while RyR is present at relatively low levels in these cells. RyR is most enriched in the dentate gyrus and CA3/4 areas of the hippocampus, where IP_3R levels are low. In the cortex, IP_3R is found in pyramidal cell bodies and proximal dendrites, whereas RyR is located predominantly in long, thin apical dendrites of pyramidal cells. In deep cerebellar nuclei, RyR is located in cell bodies that appear devoid of IP_3R, whereas IP_3R is enriched in terminals surrounding cell bodies. Electron microscopy in the hippocampus reveals RyR in axons, dendritic spines, and dendritic shafts near dendritic spines while IP_3R is primarily identified in dendritic shafts and cell bodies. These results suggest that the IP_3- and ryanodine-sensitive Ca^{2+} pools have largely distinct roles in controlling intracellular Ca^{2+} levels, though in some sites they may interact to varying degrees.

[Key words: ryanodine receptor, inositol 1,4,5-trisphosphate receptor, Ca^{2+} pumping ATPase, SERCA 2, immunohistochemistry, Ca^{2+} release]

Ca^{2+} release from endoplasmic reticulum (ER) stores is critical for the function of a wide variety of cells throughout the body, including neurons. Ca^{2+} uptake and release from intracellular stores have been best characterized in skeletal muscle. The Ca^{2+} storage organelle of skeletal muscle, the sarcoplasmic reticulum, contains a high-affinity Ca^{2+} uptake mechanism (Ca^{2+}-pumping ATPase), a low-affinity, high-capacity Ca^{2+}-binding protein (calsequestrin), and a Ca^{2+} release channel that is sensitive to caffeine and the plant alkaloid ryanodine (Fleischer and Inui, 1989). ^{3}H-ryanodine binding assays have been used to identify and purify the ryanodine receptor (RyR) from several tissues (Imagawa et al., 1987; Inui et al., 1987a,b; McPherson et al., 1991). The RyR has been cloned (Takeshima et al., 1989; Nakai et al., 1990; K. Otsu et al., 1990; Zorazto et al., 1990) and shown to function as a Ca^{2+} channel (Imagawa et al., 1987; Anderson et al., 1989; McPherson et al., 1991). Although the exact mechanism by which the striated muscle RyR is activated is unknown, in cardiac muscle, Ca^{2+} release from the sarcoplasmic reticulum through RyR is believed to be triggered by Ca^{2+} itself in a process termed Ca^{2+}-induced Ca^{2+} release (CICR) (Endo, 1977; Fabiato, 1983; Nabauer et al., 1989).

The nature of Ca^{2+} stores in neurons remains unclear in terms of their distribution, intracellular location, and biochemical composition (Burgoyne and Cheek, 1991). Neurons contain a nonmuscle form of ER Ca^{2+}-pumping ATPase (Plessers et al., 1991), as well as calsequestrin (Volpe et al., 1990) and a second Ca^{2+}-binding protein, calreticulin (Treves et al., 1990), which likely function as components of releasable Ca^{2+} pools. Ca^{2+} release from ER in neural tissues was originally characterized in relation to inositol 1,4,5-trisphosphate (IP_3) acting through a specific receptor protein, the IP_3 receptor (IP_3R), which has been purified (Supattapone et al., 1988) and cloned (Furuichi et al., 1989; Mignery et al., 1989, 1990). A second Ca^{2+} pool, sensitive to ryanodine and caffeine, has also been identified in neurons (Palade et al., 1987; Thayer et al., 1988; Glaum et al., 1990) leading to the purification of the brain RyR and the demonstration of its role as a caffeine-sensitive Ca^{2+} release channel (McPherson et al., 1991).

The relative roles of Ca^{2+} pools associated with IP_3R and RyR in regulating Ca^{2+} dynamics are unclear. In tissues that express both Ca^{2+} release channels, interactions between IP_3-sensitive and ryanodine/caffeine-sensitive Ca^{2+} pools may play a role in phenomena such as Ca^{2+} waves and Ca^{2+} oscillations

Received Aug. 25, 1992; revised Jan. 4, 1993; accepted Jan. 29, 1993.

This work was supported by U.S. Public Health Service Grant MH-18501, Research Scientist Award DA-00074 to S.H.S., and a grant of the International Life Sciences Institute. A.H.S. is supported by Postdoctoral Fellowship MH09953. T.M.D. is a Pfizer Postdoctoral Fellow and is supported by the American Academy of Neurology, the French Foundation for Alzheimer's Research, the Dana Foundation, and a Public Health Service CIDA NS01578-01. K.P.C. is an investigator of the Howard Hughes Medical Institute. C.A. is supported by U.S. Public Health Service Grants EY08055 and 2-S07-RR07062-26, NSF Presidential Faculty Fellowship.

Correspondence should be addressed to Solomon H. Snyder, Department of Neuroscience, Johns Hopkins University School of Medicine, 725 North Wolfe Street, Baltimore, MD 21205.

(Berridge, 1990). The CNS distribution of the IP_3R has been well characterized (Ross et al., 1989; Worley et al., 1989; H. Otsu et al., 1990; Satoh et al., 1990; Nakanishi et al., 1991; Sharp et al., 1993; Takei et al., 1992), and recent studies aimed at characterizing the distribution of the RyR in the CNS have been performed (Padua et al., 1992; Zupanc et al., 1992). However, the distribution of the RyR has not been determined with cellular and subcellular resolution in the mammalian brain, and the comparative localizations of the two receptors have not been well characterized except in chicken Purkinje cells (Walton et al., 1991). In an initial study to clarify the relative roles of IP_3R- and RyR-associated Ca^{2+} pools in the brain, we observed differential localizations of ER Ca^{2+} pools regulated by caffeine and IP_3 (Verma et al., 1992). In the present study, utilizing immunohistochemistry, we compare in detail at the light and electron microscopic level the localizations of IP_3R and RyR in the rat brain. In addition, we have compared the distributions in the brain of these Ca^{2+} release channels with the distribution of the major Ca^{2+}-pumping ATPase, SERCA 2.

Materials and Methods

Preparation of antibodies

Affinity-purified rabbit anti-IP_3R (AP2A) was prepared exactly as described previously (Sharp et al., 1993). Antibody GP-561 was prepared by immunizing a guinea pig with purified brain RyR (approximately 10 μg/injection) prepared as described (McPherson et al., 1991) and mixed 1:1 with Freund's complete adjuvant. The animal was boosted on days 14, 28, and 56 with purified receptor in Freund's incomplete adjuvant. Serum was monitored for anti-RyR antibodies by immunoblot analysis using purified brain RyR. Anti-RyR antibodies were affinity purified against cardiac RyR purified from cardiac microsomes as described for purification of brain RyR (McPherson et al., 1991) except that the DEAE-agarose step was omitted. The purified cardiac RyR was subjected to SDS-PAGE and transferred to polyvinylidinedifluoride (PVDF) membranes (Towbin et al., 1979). A strip of PVDF membrane containing the cardiac RyR was cut from the blot and used for affinity purification. The serum was incubated for 16 hr at 4°C with blot strips containing 750 μg of cardiac RyR. The PVDF membrane strips were washed 4 × 10 min in 50 mM Tris-HCl (pH 7.4) containing 500 mM NaCl followed by a 10 min wash in 50 mM Tris-HCl (pH 7.4), 100 mM NaCl. Antibody was eluted by incubating the strips for 15 min in 100 mM glycine (pH 2.5), followed by pH neutralization with Tris. Antibodies were then dialyzed for 12 hr against PBS containing 20% sucrose, 1 mM EDTA, and 0.001% sodium azide. Monoclonal antibody IID8 against the canine cardiac ATPase was prepared as previously described (Jorgenson et al., 1988).

Membrane preparation and Western blot analysis

To prepare membranes for immunoblots, whole rat brains were cut into small pieces and placed in 10 vol of 20 mM HEPES (pH 7.4), containing 0.32 M sucrose and a cocktail of protease inhibitors (McPherson and Campbell, 1990). The tissue was homogenized using 10 strokes by hand in a glass–Teflon homogenizer. The homogenate was centrifuged at 1000 × *g* for 10 min and the pellet discarded. The supernatant was centrifuged for 13 min at 26,000 × *g* and the pellet again discarded. The supernatant was centrifuged for 45 min at 186,000 × *g*, and the microsomal membranes were collected and resuspended in the same buffer used for homogenization. Membrane proteins were resolved on 3–12% SDS-polyacrylamide gels (Laemmli, 1970) and transferred to nitrocellulose paper (Towbin et al., 1979). The blots were blocked with 3% bovine serum albumin (BSA) in 50 mM Tris-HCl (pH 7.4), 1.5% NaCl (TBS) for 1 hr before overnight incubation with antibodies. The blots were then washed, incubated for 1 hr with horseradish peroxidase–labeled secondary antibodies, washed again, and developed using 4-chloro-1-naphthol and H_2O_2 for AP2A and the Visi-Blot immunodetection system (U.S. Biochemicals) for GP-561.

Immunocytochemistry

Light microscopy. Rats were anesthetized deeply with sodium pentobarbital and perfused with 50 ml of ice-cold 50 mM sodium phosphate (pH 7.4), 0.9% NaCl (PBS) followed by 200–300 ml of cold 4% paraformaldehyde, 0.1% glutaraldehyde in 100 mM sodium phosphate (pH 7.4). Tissue was then removed and further fixed by incubation in the same solution without glutaraldehyde for 4 hr at 4°C. Tissue was then cryoprotected by overnight incubation in 20% glycerol in 100 mM sodium phosphate (pH 7.4). After freezing the tissue with dry ice, sections (40 μm thick) were cut into cold TBS using a sliding microtome. The free-floating sections were stored at −20°C in an antifreeze solution [10% (w/v) PVP-40, 30% (w/v) sucrose, 10% (v/v) ethylene glycol, and 50 mM sodium phosphate (pH 7.4)]. Before staining, sections were rinsed in TBS and permeabilized with 0.2% Triton X-100 in TBS for 30 min. Sections were then blocked by incubation in TBS containing 5% normal serum from the same species as the secondary antibodies. The sections were incubated overnight at 4°C, with gentle agitation with primary antibodies in TBS containing 1.5% normal serum from the same species as the secondary antibody. Affinity-purified anti-IP_3R (AP2A) was used at approximately 1 μg/ml, affinity-purified anti-RyR (GP561) was used at 1:50 dilution, and monoclonal anti-Ca^{2+} pump (IID8) culture supernatant was used at a dilution of 1:10. The sections were then washed 3 × 10 min in TBS containing 1% normal serum and incubated for 1 hr at room temperature with the appropriate biotin-conjugated secondary antibody (goat anti-rabbit IgG at 1:200 dilution, goat anti-guinea pig IgG at 1:200 dilution, or rat-adsorbed horse anti-mouse at 1:100 dilution from Vector Laboratories) in TBS containing 1.5% normal serum from the appropriate species. After three 10 min washes in TBS, sections were incubated with an avidin–biotin–peroxidase complex (Vector Elite, 1:50 dilution; Vector Laboratories) in TBS for 45 min at room temperature. The sections were then washed 3 × 10 min in TBS before development with a substrate solution consisting of 0.01% H_2O_2 and 0.5 mg/ml diaminobenzidine in TBS. Sections were rinsed with TBS and mounted on subbed glass slides. After dehydration in graded alcohol solutions, the sections were coverslipped with Permount (Fisher). For fluorescence immunocytochemistry, the sections were treated as above through the primary incubations except that the primary incubation mixture contained both AP2A and GP561 at the same dilutions used above. Sections were then incubated for 1 hr at room temperature in a 1:100 dilution of rhodamine-conjugated donkey anti-rabbit IgG (Jackson Immunoresearch) plus 1:200 biotinylated anti-guinea pig IgG in TBS plus 1.5% normal goat serum. After washing 3 × 10 min in 1% normal goat serum, the sections were incubated for 1 hr at room temperature in fluorescein-conjugated avidin-cell sorter grade (DCS) (Vector Laboratories) in TBS plus 1.5% normal goat serum. Sections were then washed as above, incubated for 1 hr in a 1:200 dilution of goat anti-avidin (Vector) in the same medium used above, washed again, and incubated again for 1 hr in a 1:100 dilution of fluorescein-conjugated avidin DCS. Sections were then washed in TBS, rinsed briefly in distilled water, and mounted in Mowiol mounting medium (Heimer and Taylor, 1974) containing 7.5 μg/ml *n*-propyl gallate (Giloh and Sedat, 1982) before viewing with the appropriate filters on a Zeiss Axioplan microscope.

Electron microscopy. Adult (200–300 gm) Sprague–Dawley male rats were deeply anesthetized with sodium pentobarbital, and then perfused transcardially with heparinized saline followed by 50 ml of 3.75% acrolein, 2% paraformaldehyde (King et al., 1983), 100 mM sodium phosphate (pH 7.3), and then with 200 ml of 2% paraformaldehyde in 100 mM sodium phosphate (pH 7.4). Alternatively, anesthetized rats were perfused with 500 ml of 4% paraformaldehyde in 100 mM sodium phosphate (pH 7.4). Brains were removed from the skull and sliced into 2-mm-thick coronal slabs. The slabs were postfixed by immersion for another 30 min in 2% or 4% paraformaldehyde in 100 mM sodium phosphate (pH 7.4). Sections (40 μm thick) were cut from a slab of tissue containing the dorsal hippocampus using a Vibratome and collected into 100 mM sodium phosphate (pH 7.4). The cross-linking action of acrolein was terminated by immersing the sections for 30 min in 1% $NaBH_4$ in 100 mM sodium phosphate (pH 7.4) and then rinsing repeatedly in 100 mM sodium phosphate (pH 7.4) alone until bubbles ceased to emerge from the sections. Sections were then transferred to buffer consisting of 100 mM Tris-HCl (pH 7.4) and 0.9% NaCl and immersed for 30 min in the same buffer containing 1% BSA. Free-floating sections were incubated overnight at room temperature with continuous agitation in the anti-IP_3R or anti-RyR antibody solutions in 1% BSA in 100 mM Tris-HCl (pH 7.4), 0.9% NaCl. This and all other incubations were terminated by rinsing for 10 min in 100 mM Tris-HCl, 0.9% NaCl. On the following day, sections immersed in anti-IP_3R antibodies were incubated for 30 min in biotinylated goat anti-rabbit IgG antibody (Vector Laboratories) diluted 1:200 in 100 mM Tris, 0.9%

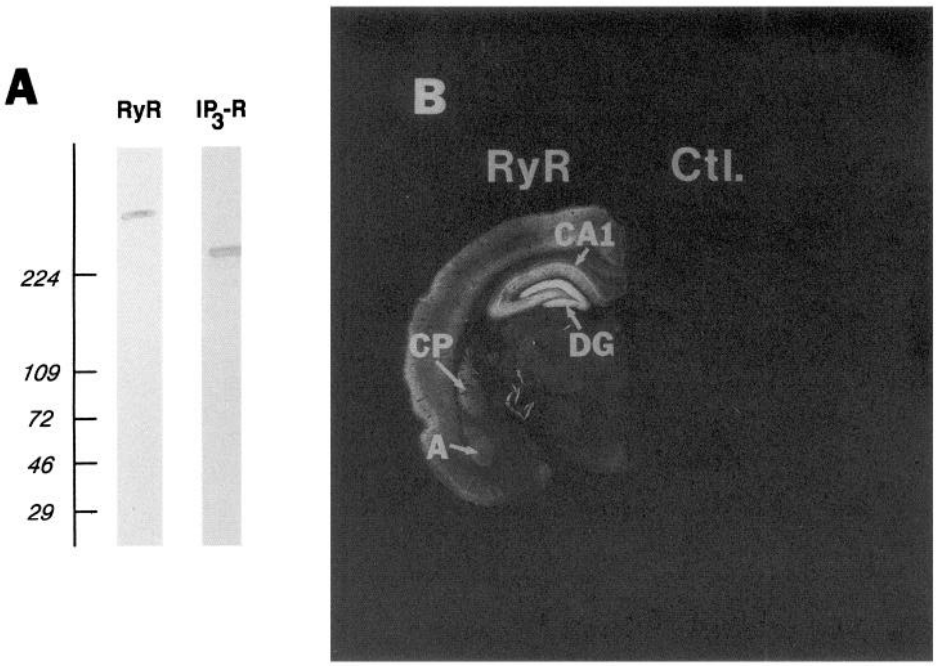

Figure 1. Specificity of affinity-purified antibodies against RyR and IP_3R. *A*, Brain microsome proteins (250 μg) were resolved on 3–12% SDS-polyacrylamide gels. Proteins were transferred to nitrocellulose paper and stained with affinity-purified antibodies against the brain ryanodine receptor (*RyR*) or IP_3 receptor (*IP_3R*) as described in Materials and Methods. The positions of the molecular weight standards are indicated on the *left*. *B*, Dark-field photomicrographs illustrating the specificity of the antibodies to RyR. In this reproduction, dense labeling appears bright against a dark background. The *left panel* (*RyR*) shows staining with antibodies against RyR while the *right panel* (*Ctl.*, control) shows staining after preadsorption of anti-RyR antibodies with immobilized RyR. *A*, amygdala; *CA1*, CA1 field of Ammon's horn of the hippocampus; *CP*, caudate putamen; *DG*, dentate gyrus.

NaCl, 1% BSA. Sections immersed in the anti-RyR antibodies were incubated for 30 min in biotinylated donkey anti-guinea pig IgG antibody (Jackson InmmunoResearch) diluted 1:50 in the same buffer. Upon completion of this incubation, sections were immersed for 30 min in 100 mM Tris-HCl (pH 7.4) containing avidin–biotin–peroxidase complex (Vector Laboratories), and then reacted for 6 min in peroxidase substrate solution consisting of 22 mg of 3,3′-diaminobenzidine tetrahydrochloride and 10 μl of 30% H_2O_2 in 100 ml of 100 mM Tris-HCl (pH 7.4). After rinsing with 100 mM Tris-HCl, 0.9% NaCl, sections were immersed in 100 mM sodium phosphate (pH 7.4) and then prepared for electron microscopic analyses as follows.

Paraformaldehyde-fixed sections were postfixed for 10 min in 2.5% glutaraldehyde buffered with 10 mM sodium phosphate, 0.9% NaCl. All sections were further postfixed for 1 hr in 2% OsO_4 in 100 mM sodium phosphate (pH 7.4), and then dehydrated using increasing concentrations of ethanol. Sections were then immersed for 2 × 10 min in acetone, infiltrated overnight with Epon 812 (Electron Microscopy Sciences) diluted 1:1 with acetone, and then infiltrated for 2 hr with 100% Epon. Sections were sandwiched between two sheets of Aclar plastic (Masurovsky and Bunge, 1968) and cured overnight at 60°C. On the following day, the flat-embedded sections were examined under the light microscope to choose areas for electron microscope sampling, cut out with scissors, and reembedded in capsules. Half of the ultrathin sections were counterstained with uranyl acetate and lead citrate while the others were left uncounterstained. Sections capturing the Epon–tissue interface of all regions of the hippocampus were examined using the JEOL 1200XL electron microscope at magnifications ranging from 2000× up to 30,000×. Further details of electron microscopic immunocytochemical methods have been described previously (Chan et al., 1990).

Results

Specificity of antisera

To ascertain the specificity of the antisera employed, we conducted Western blot analysis of whole-brain microsomal fractions (Fig. 1*A*). Both anti-IP_3R and anti-RyR antibodies stain single immunoreactive bands at the approximate molecular masses of 260 kDa for IP_3R and 565 kDa for RyR. Immunoperoxidase staining of rat brain sections with affinity-purified GP561 antibodies against the RyR (Fig. 1*B*, RyR) shows regional heterogeneity and the staining is eliminated by preadsorption with highly purified RyR (Fig. 1*B*, Ctl.) demonstrating specificity of the antibodies. The affinity-purified polyclonal rabbit anti-IP_3R antibodies (AP2A) have been previously characterized (Sharp et al., 1993). The monoclonal antibody IID8 against the Ca^{2+} pump used in this study has also been extensively characterized and used for immunoblot and immunohistochemical studies on brain cerebellar tissue (Jorgenson et al., 1988; Plessers et al., 1991; Spencer et al., 1991).

Immunohistochemical localization of IP_3R, Ca^{2+} pump, and RyR

Clear differences in the localization of IP_3R and RyR are evident both in sagittal and in coronal sections (Figs. 2, 3). For instance, in the hippocampus IP_3R is most concentrated in pyramidal cells of CA1, with substantially lesser densities in CA3 and only moderate levels in the granule cells of the dentate gyrus (see also Fig. 4). By contrast, RyR staining is much greater in CA3 than CA1 and is particularly prominent in the granule cell layer of the dentate gyrus. The thalamus is enriched in IP_3R except for the anterior dorsal nucleus, which is notably deficient. On the other hand, RyR density is very low in the thalamus. The corpus striatum, on the other hand, displays similar levels of RyR and IP_3R staining. The substantia nigra displays much higher levels of IP_3R than RyR.

Some brain regions possess high levels of both IP_3R and RyR but in different locations. For instance, the entire lateral septum, including the dorsal and intermediate divisions, is enriched in RyR, while IP_3R levels are high only in a select population of cells in the intermediate lateral septum. In the olfactory bulb, RyR is densest in the dendrites of mitral cells in the external plexiform layer, a zone that is relatively devoid of IP_3R. Granule cells and their dendrites also stain positive for the RyR. On the other hand, IP_3R is concentrated in periglomerular cells in the glomerular layer and in granule cells in the mitral cell and granule cell layers (Fig. 2; Sharp et al., 1993).

The anterior olfactory cortex possesses high densities of IP_3R with very low levels of RyR. By contrast, the islands of Calleja are devoid of IP_3R but possess moderate levels of RyR. In the retrosplenial cortex, marked differences in the layering of RyR

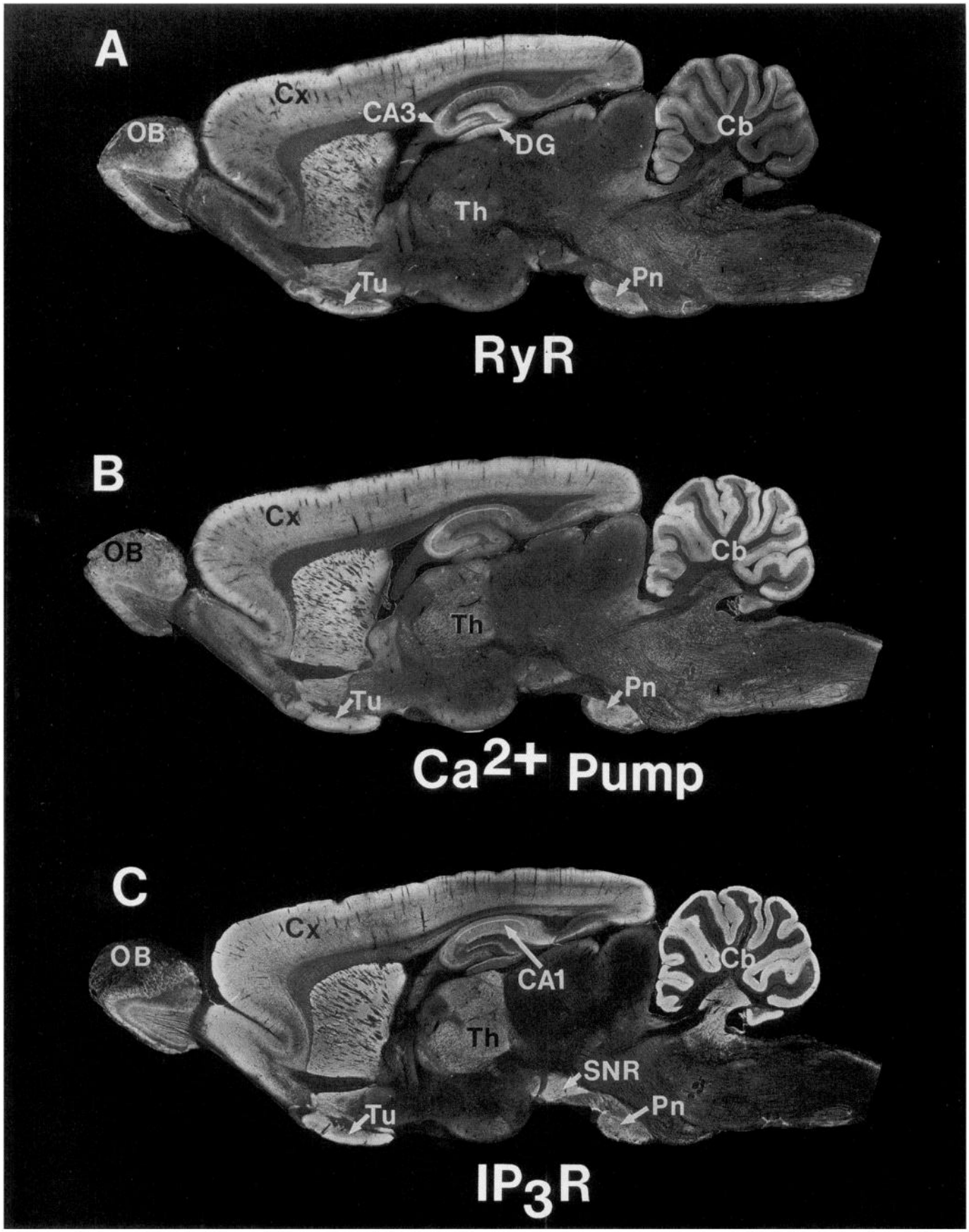

Figure 2. Serial sagittal sections demonstrating the overall distribution of RyR (*A*), Ca^{2+} pump (*B*), and IP_3R (*C*) in rat brain. In these dark-field photomicrographs, dense labeling appears bright against a dark background. *OB*, olfactory bulb; *Cx*, cortex; *CA1–CA3*, fields of Ammon's horn of the hippocampus; *DG*, dentate gyrus; *Tu*, olfactory tubercle; *Th*, thalamus; *Pn*, pontine nuclei; *Cb*, cerebellum; *SNR*, substantia nigra pars reticulata.

and IP_3R are evident in coronal sections (Fig. 3*D,F*; see Fig. 6*A,B*).

Ca^{2+} pump immunoreactivity throughout the brain labels sites of both RyR and IP_3R, although in general the pattern of Ca^{2+} pump immunoreactivity tends to match the distribution of IP_3R better than RyR.

High-power light microscopic comparison of IP_3R and RyR

Differences in IP_3R and RyR localization at the cellular level are evident under high-power magnification (Figs. 4, 5). In the cerebellum both IP_3R and RyR as well as the Ca^{2+} pump are localized to Purkinje cells and their dendritic trees, with IP_3R being especially prominent. Marked differences in the localizations of IP_3R and RyR are evident in deep nuclei of the cerebellum. As reported previously, IP_3R immunoreactivity is concentrated in punctate nerve terminals surrounding large cell bodies (Fig. 4; Mignery et al., 1989; Sharp et al., 1993). On the other hand, RyR is localized exclusively to neuronal cell bodies. Ca^{2+} pump immunoreactivity occurs most prominently in cells with only weak staining visible in neuropil in the deep cerebellar nuclei.

In the hippocampus, high-power views confirm the striking differences in RyR and IP_3R that were evident at lower magnifications (Fig. 4). Specifically, IP_3R is highly concentrated in pyramidal cells of CA1 with much lower densities in CA3 and the dentate gyrus. RyR displays an inverse pattern in that the highest concentrations are in the dentate gyrus and CA3 regions. Ca^{2+} pump immunoreactivity is evident throughout the hippocampus but is highest in the CA3 region and is comparatively less dense in the dentate gyrus than RyR and less dense in the CA1 region that the IP_3R.

High-power microscopy of the substantia nigra shows substantial differences in the cellular distribution of RyR and IP_3R. IP_3R is concentrated in terminals, consistent with earlier studies (Worley et al., 1989), while RyR is densest in cell bodies of interneurons within the zona reticulata.

High-power evaluation of the cerebral cortex differentiates cellular patterns for IP_3R and RyR (Fig. 5). In the motor cortex IP_3R immunoreactivity is most prominent in cell bodies and their proximal dendrites in superficial, intermediate, and deeper layers. By contrast, in all of these layers RyR is most evident in long, thin dendritic processes, with little immunoreactivity in cell bodies. The pattern of Ca^{2+} pump immunoreactivity tends to resemble most that of IP_3R, though for the Ca^{2+} pump, immunoreactivity is greatest in cells in the intermediate layers.

In the posterior parietal cortex similar differences in IP_3R and RyR are evident. In superficial layers IP_3R is concentrated in the perikarya and proximal dendrites of pyramidal cells while in deeper cells very intense staining is evident in a population of nonpyramidal cells. On the other hand, RyR is most evident in long, thin dendrites with much less cellular immunoreactivity. Ca^{2+} pump immunoreactivity closely resembles IP_3R in the pyramidal cells in more superficial layers with less staining than IP_3R in the nonpyramidal cells of deeper layers.

To ascertain whether IP_3R and RyR might be colocalized in the same cells in certain areas, we conducted some double-labeling studies (Fig. 6). In the CA1 layer of the hippocampus IP_3R and RyR appear to be localized to many of the same pyramidal cells with virtually identical patterns of immunoreactivity in dendrites. On the other hand, in the retrosplenial cortex distinct differences are evident. Thus, RyR is concentrated in pyramidal cells and their dendrites in a relatively deep layer, while IP_3R is evident in a different population of pyramidal cells in a more superficial layer.

Electron microscopic analysis

Light microscopic immunocytochemistry revealed high levels of IP_3R in the CA1 region of the hippocampus while RyR labeling was enriched in the CA3 region and the dentate gyrus. Thus, electron microscopic analysis focused upon the hippocampal formation (Fig. 7). IP_3R immunolabeling occurs in a subpopulation of dendritic profiles throughout the various regions of the hippocampus, while immunolabeling within axons and axon terminals is weak or not detectable. Figure 7*A* shows representative IP_3R immunoperoxidase labeling in dendrites of the CA1 region. Within dendrites, IP_3R labeling occurs most prominently in dendritic shafts, but labeled dendritic spines are also occasionally observed. Labeling of spines is usually weak relative to labeling in dendritic shafts. RyR labeling occurs in dendrites (Fig. 7*B*), axons (Fig. 7*C*), and a number of small-diameter profiles that are not readily identified as dendritic, axonal, or glial. RyR labeling is notable in dendritic spines in various regions of the hippocampus including the dentate gyrus, CA1, CA3, and hilar regions. Prominent RyR labeling is observed in spines that are contiguous with unlabeled dendritic shafts (Fig. 7*B*). Dendritic shafts are mostly unlabeled except for patches at points of emergence of spines. Within dendrites, intense RyR immunoreactivity is associated with saccules near the plasma membrane.

Discussion

The most striking finding of the present study involves the contrasting localizations of IP_3R and RyR. The regional differences we have observed by light microscopic immunohistochemistry correspond well with similar differences observed in our earlier studies labeling ER pools of Ca^{2+} with $^{45}Ca^{2+}$ and monitoring differential release of radiolabel by IP_3 and caffeine, which selectively influence the IP_3-sensitive Ca^{2+} pool and the ryanodine-sensitive CICR pool of Ca^{2+}, respectively (Verma et al., 1992). The regional localization of the RyR is also in general agreement with the results of Padua et al. (1992), who recently localized RyR to various regions of the rat brain by autoradiographic methods. Thus, the relative prominence of the two types of Ca^{2+} release appears to vary in different brain regions. Different localizations of IP_3R and RyR are evident both for relatively large brain areas such as the CA1–CA4 fields and lamina of the hippocampus as well as at a cellular level, such as differences in relative labeling of perikarya and dendrites in the cerebral cortex.

In the hippocampus, using double labeling, we show that some cells possess both IP_3R and RyR. This finding fits with observations of others (Walton et al., 1991) who demonstrated both RyR and IP_3R immunoreactivity in the same Purkinje cells of the chicken cerebellum. It has been suggested that in many cells the IP_3 and CICR processes of Ca^{2+} release operate in close coordination with IP_3 releasing Ca^{2+} to trigger the CICR process via the RyR (Berridge and Galione, 1988; Goldbeter et al., 1990; Harootunian et al., 1991; Randriamampita et al., 1991; Tsunoda, 1991). These interactions can lead to a variety of phenomena including Ca^{2+} waves and Ca^{2+} oscillations. However, in vertebrate eggs, Ca^{2+} oscillations and waves can be generated by a mechanism involving IP_3-sensitive Ca^{2+} stores in the absence of RyR (Miyazaki et al., 1992; Parys et al., 1992). In neurons, including hippocampal pyramidal neurons, most ev-

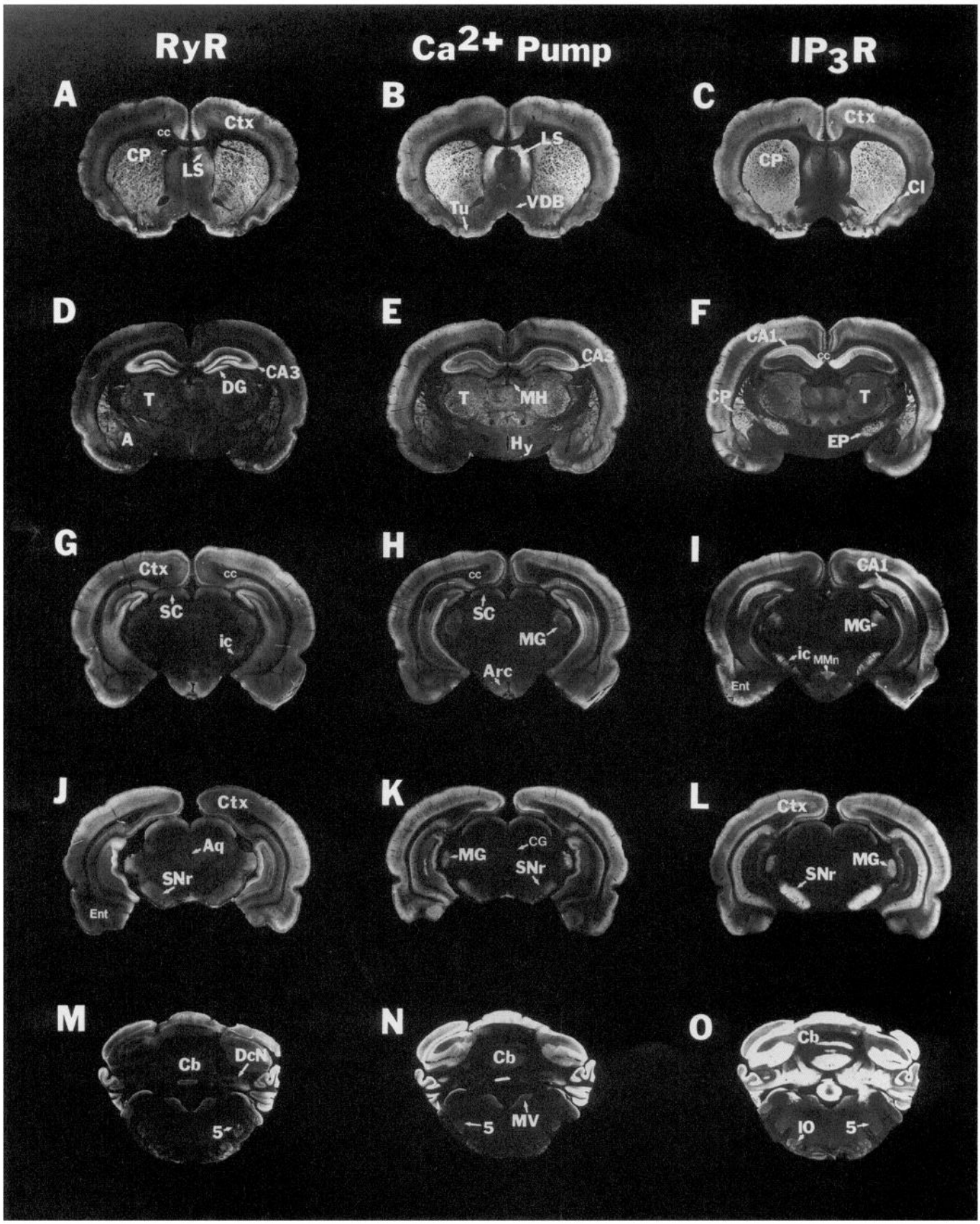

Figure 3. Low-power dark-field photomicrographs of serial sections of rat brain stained with antibodies for RyR (*A, D, G, J, M*), Ca^{2+} pump (*B, E, H, K, N*), and IP_3R (*C, F, I, L, O*) presenting an alternate view of the relative distributions and density of the three proteins throughout the rat brain. *Ctx*, cortex; *cc*, corpus callosum; *CP*, caudate putamen; *LS*, lateral septum; *Tu*, olfactory tubercle; *VDB*, vertical limb of the diagonal band of Broca; *Cl*, claustrum; *CA1–CA3*, fields of Ammon's horn of the hippocampus; *A*, amygdala; *T*, thalamus; *DG*, dentate gyrus; *MH*, medial habenula; *Hy*, hypothalamus; *EP*, entopeduncular nucleus; *SC*, superior colliculus; *ic*, internal capsule; *Arc*, arcuate nucleus; *MG*, medial geniculate; *Ent*, entorhinal cortex; *MMn*, medial mammillary nucleus; *Aq*, cerebral aqueduct; *SNr*, substantia nigra pars reticulata; *CG*, central gray; *Cb*, cerebellum; *5*, cranial nerve 5; *DcN*, deep cerebellar nuclei; *MV*, medial vestibular nucleus; *IO*, inferior olive.

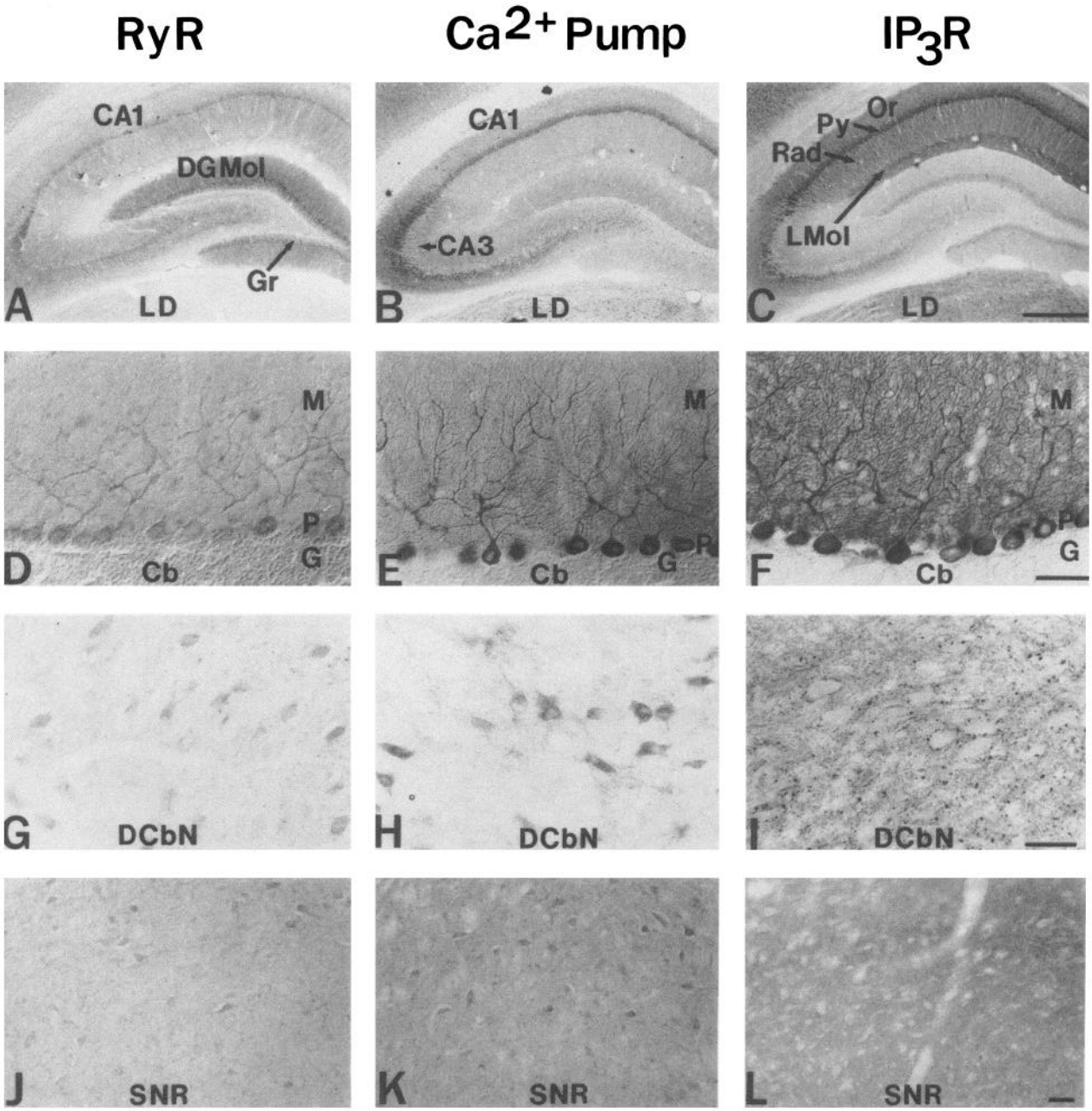

Figure 4. Bright-field photomicrographs demonstrating the pattern of immunoreactivity of RyR (*A, D, G, J*), Ca^{2+} pump (*B, E, H, K*), and IP_3R (*C, F, I, L*) in various regions of the rat brain. Note the contrast in the distribution and relative intensity of labeling of RyR (*A*), and IP_3R (*C*) in the hippocampal formation. In the cerebellum (*Cb*), all three antibodies have a similar pattern, but vary in intensity (*D–F*). IP_3R (*I*) in the deep cerebellar nuclei (*DCbN*) is primarily localized to the neuropil and there is a relative lack of staining of perikarya. This contrasts with the staining of cell bodies by RyR (*G*) and Ca^{2+} pump (*H*) in the deep cerebellar nuclei. A similar pattern of staining to that in the deep cerebellar nuclei for all three antibodies is present in the substantia nigra reticulata (*SNR*) (*J–L*). *CA1–CA3*, fields of Ammon's horn of the hippocampus; *DG Mol*, molecular layer of the dentate gyrus; *Gr*, granule cell layer of the dentate gyrus; *LD*, lateral dorsal thalamic nucleus; *LMol*, lacunosum moleculare of the hippocampus; *Or*, stratum oriens of the hippocampus; *Py*, pyramidal cell layer of the hippocampus; *Rad*, stratum radiatum of the hippocampus; *M*, molecular layer of the cerebellum; *P*, Purkinje cell layer of the cerebellum; *G*, granule cell layer of the cerebellum.

idence suggests that the two Ca^{2+} pools are functionally distinct (Thayer et al., 1988; Murphy and Miller, 1989; Glaum et al., 1990), although cerebellar granule cells are an apparent exception (Irving et al., 1992). In addition, there is evidence that in neurons oscillations of internal Ca^{2+} can be generated from a single caffeine-sensitive store (Friel and Tsien, 1992a,b). Our data show that if interactions between the two stores do occur, then the relative roles of the two systems must differ substantially in various brain regions and cell types as well as within individual cells.

While Scatchard analysis showed that the B_{max} for IP_3R is nearly 10 times the B_{max} for RyR in the brain (data not shown; McPherson and Campbell, 1990; Padua et al., 1991), it should be emphasized that the unit conductance for RyR channels is about 10 times the unit conductance for IP_3R channels (Ehrlich and Watras, 1988; McPherson et al., 1991). Thus, the overall

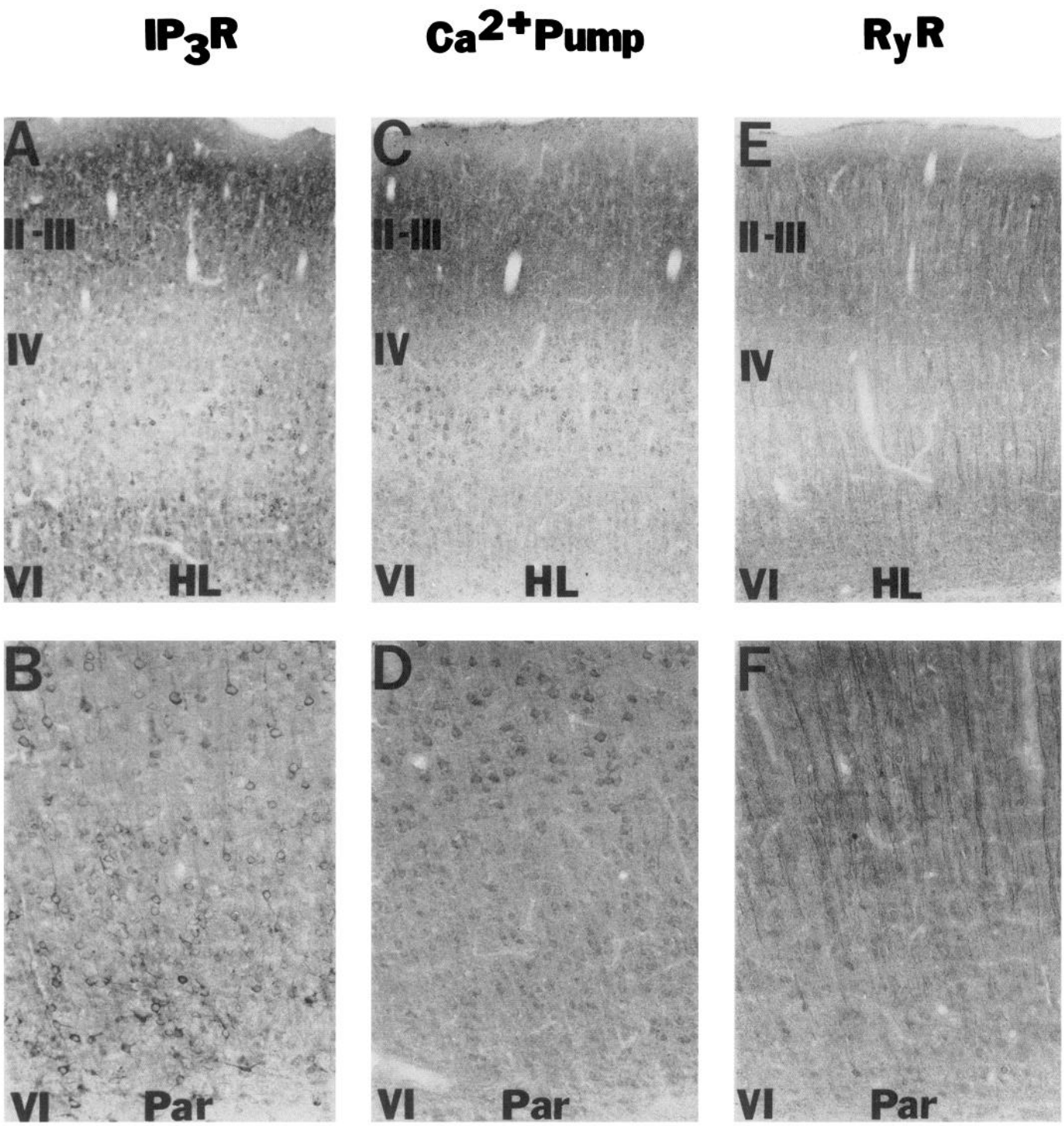

Figure 5. High-power reproductions of the staining pattern for antibodies to IP_3R (*A, B*), Ca^{2+} pump (*C, D*), and RyR (*E, F*) in the hindlimb (*HL*) motor cortex and in the parietal cortex (*Par*). Note the contrasting pattern of staining of all three antibodies within the various layers (*II–IV*) of the cortices.

amount of Ca^{2+} release associated with IP_3 and CICR processes may be fairly similar. This would fit with our observations that $^{45}Ca^{2+}$ release in brain slices by IP_3 and the CICR processes is approximately the same (Verma et al., 1992).

At the electron microscopic level, RyR is detected in both dendrites and axons. Interestingly, RyR appears to be relatively enriched in dendritic spines in the hippocampus while IP_3R labeling in spines appears to be weak relative to labeling in dendritic shafts (Fig. 7). This finding contrasts with observations in the chicken cerebellum, where the IP_3R, but not RyR, were found to be present in dendritic spines of Purkinje cells, although both proteins were localized to dendritic shafts and perikarya of these cells (Ellisman et al., 1990; Walton et al., 1991). Recent observations in gymnotiform fish have also shown the absence of RyR in spines of cerebellar Purkinje cells (Zupanc et al., 1992). Because of the unique features of Ca^{2+} disposition in the

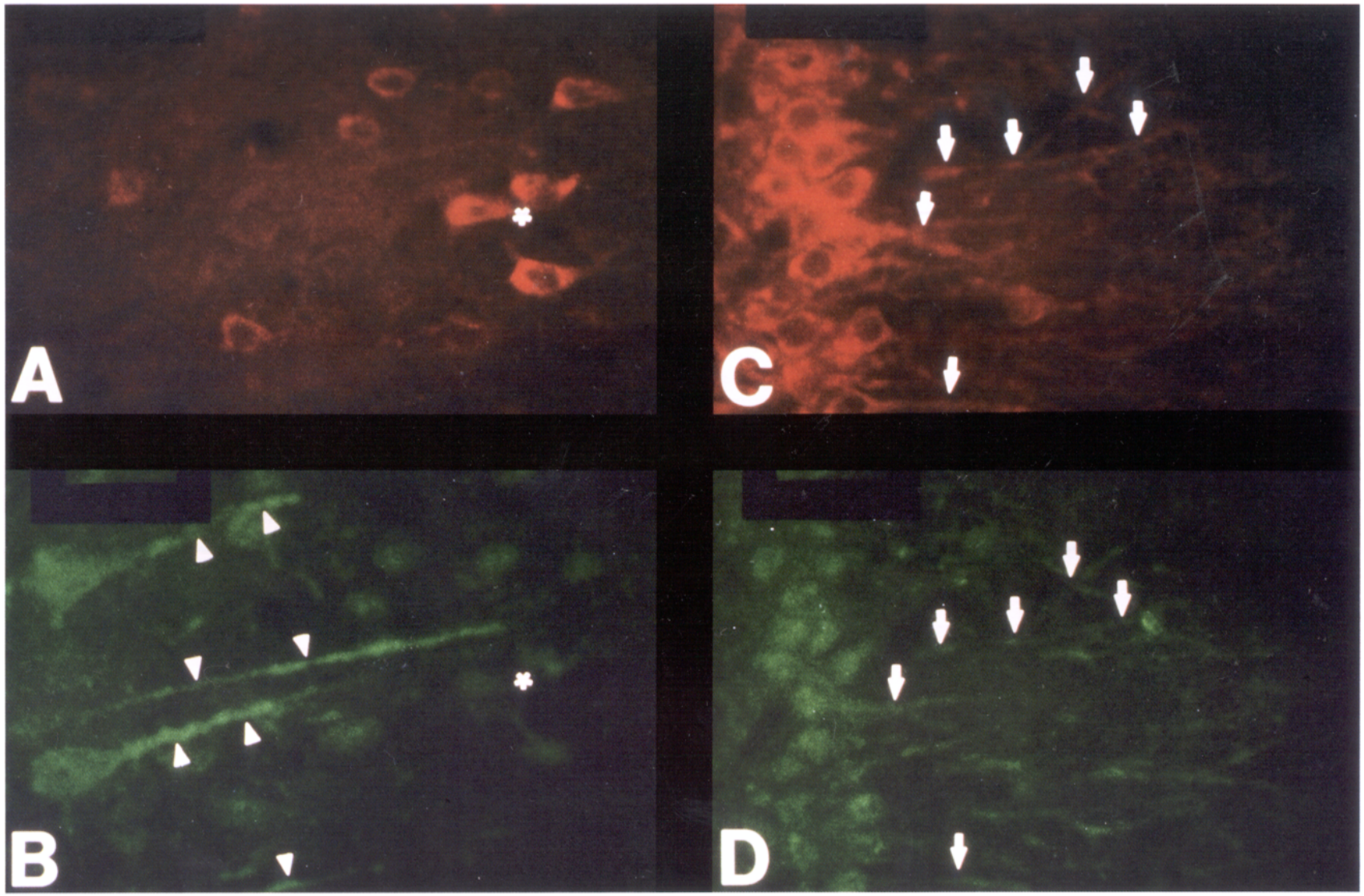

Figure 6. IP_3R (*A, C*) and RyR (*B, D*) are colocalized within individual neurons and dendrites of the retrosplenial cortex (*A, B*) and CA1 region of the hippocampus (*C, D*) as well as having contrasting localizations. Rat brain sections were stained for both IP_3R and RyR as described in Materials and Methods. IP_3R was localized using rhodamine-conjugated secondary antibodies (*A, C*). RyR was localized using biotinylated secondary antibodies followed by fluorescein-conjugated avidin, biotinylated anti-avidin, and fluorescein-conjugated avidin again. Under these conditions, staining for RyR in cell bodies was partially nonspecific while staining for RyR in processes and staining of IP_3R in general appeared completely specific (data not shown). In *A*, IP_3R staining is evident in a number of pyramidal neurons (see *asterisk*) that have a relative lack of RyR immunoreactivity (*B, asterisk*). In *B*, large pyramidal neurons in the retrosplenial cortex exhibit intense staining with RyR in dendrites (*arrowheads*), but there is a relative lack of IP_3R immunoreactivity in the same dendrites. *C* and *D* illustrate the colocalization of IP_3R and RyR, respectively, within dendrites of pyramidal neurons of CA1 of the hippocampus (*arrows*).

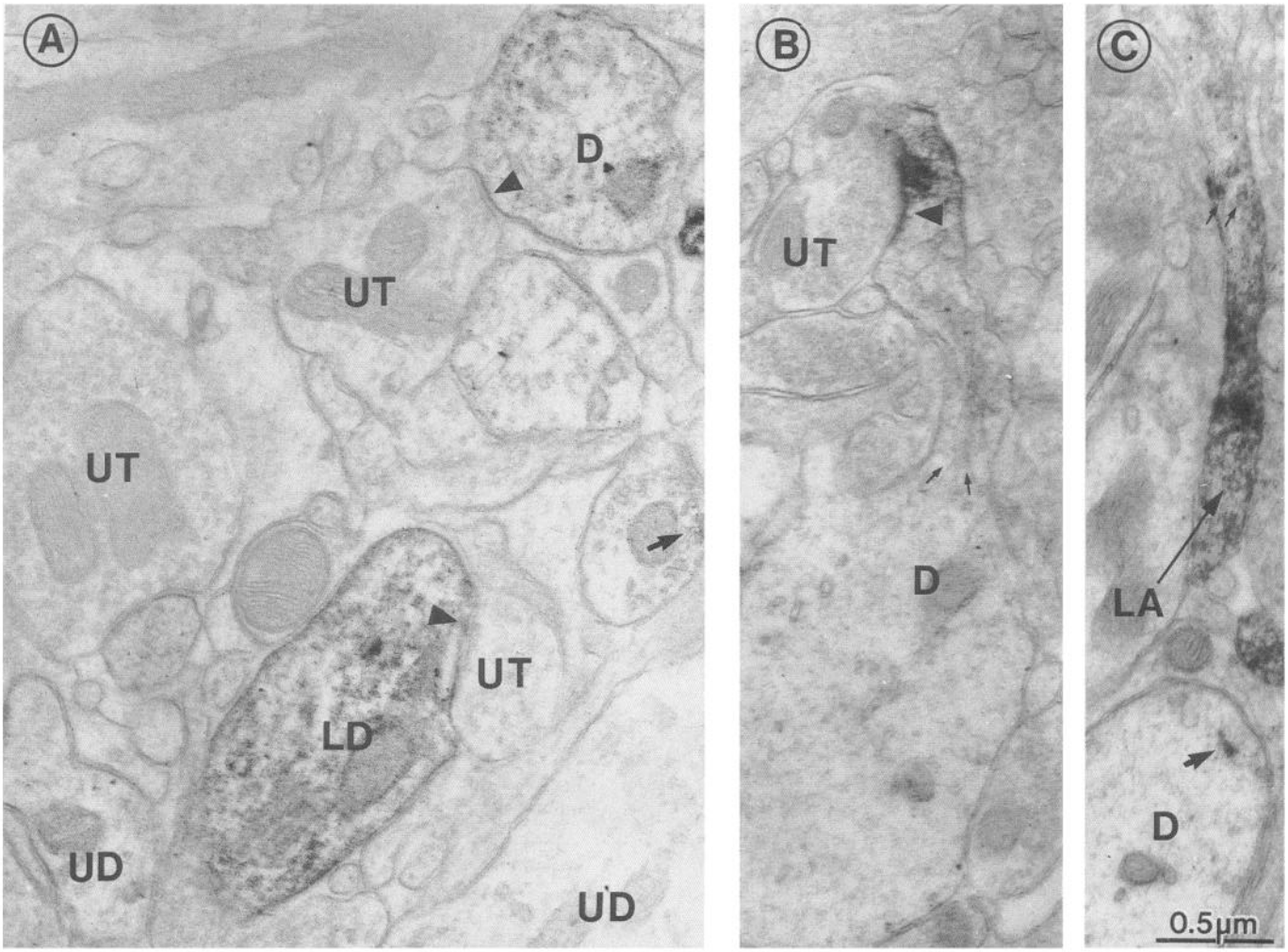

Figure 7. Ultrastructural localization of IP_3R (*A*) and ryanodine receptors (*B, C*) in hippocampal formation of the rat. All electron micrographs were taken from noncounterstained ultrathin sections so as to facilitate visualization of immunoperoxidase labeling. *A*, The electron micrograph shows immunolabeling of the IP_3R in the stratum radiatum of the hippocampal CA1 region. Immunoreactivity is prominent in one dendritic profile, *LD*, but is also apparent in others (*D*; arrowheads point to postsynaptic membranes). Dendrites with no apparent labeling are indicated as *UD* within the cytoplasm. Terminals in the vicinity are unlabeled (*UT*) except for one that shows slight labeling around vesicles (*arrow*). A spine that is postsynaptic to the *leftmost UT* (to the left of *LD*) appears lightly labeled. *B*, RyR immunoreactivity is prominent in a dendritic spine of the hilus. *Arrowhead* points to the plasma membrane that is postsynaptic to an unlabeled terminal (*UT*) while the *two small arrows* point to one end of the spine apparatus and where the spine emerges from the dendritic shaft (*D*). *C*, RyR labeling is present within an axon (*LA*). *Small arrows within LA* point to immunoreactive vesicles. A dendrite (*D*) in its vicinity also shows a discrete cluster of immunoreactivity near the plasma membrane (*arrow*).

Purkinje cells, it is not surprising that the intracellular loci of IP_3R and RyR in these cells differ from intracellular loci in other parts of the brain.

It was recently demonstrated that free cytosolic Ca^{2+} concentrations in individual dendritic spines of hippocampal pyramidal cells can be regulated somewhat independently (Guthrie et al., 1991; Muller and Connor, 1991). In response to stimulation of the associative–commissural pathway, Ca^{2+} in dendritic spines of CA3 pyramidal neurons rose to higher levels than in the dendritic shaft and stayed elevated for longer periods of time (Muller and Connor, 1991). Moreover, the results of others (Friel and Tsien, 1992a,b) have shown that a caffeine-sensitive CICR process can produce regenerative Ca^{2+} oscillations in neurons. Thus, our data support the suggestion (Miller, 1992) that a CICR process, preferentially localized to the dendritic spine, may boost the magnitude and duration of the spine Ca^{2+} signal during such processes as long-term potentiation of synaptic efficacy in the hippocampus. A preference for an RyR-based process in these spines might be explained by the findings that the diffusion coefficient of intracellular Ca^{2+}, as determined in *Xenopus* oocytes, is much slower than that of IP_3 (Meyer, 1991; Allbritton et al., 1992). This suggests that a CICR process might be better suited to produce highly localized increases in Ca^{2+} levels over extended time periods than an IP_3-based system.

In general, the localizations of Ca^{2+} pump immunoreactivity resemble both those of IP_3R and RyR, consistent with the ER Ca^{2+} pump providing the Ca^{2+} stores released both by IP_3 and by the CICR process. There is a tendency for Ca^{2+} pump localizations to fit better with IP_3R than RyR localizations, which might reflect the greater density of IP_3R than RyR that we observed in binding studies for the whole brain (not shown). However, in a number of areas, where IP_3R density is quite high, levels of Ca^{2+} pump are relatively low. These areas include

deep layers in the cerebral cortex, terminals in the deep cerebellar nuclei and, to a lesser extent, terminals in the substantia nigra. The reason for these apparent discrepancies is not presently clear, but might be accounted for by the presence of Ca^{2+} pump isoforms not detected by the monoclonal anti-Ca^{2+} pump antibody used in these studies. Known isoforms of the intracellular Ca^{2+} pump have been designated SERCAs 1, 2A, 2B, and 3 (Burk et al., 1989). We showed that the SERCA 2B isoform accounts for the bulk of the intracellular Ca^{2+} pump in the brain and localized SERCA 2B mRNA by *in situ* hybridization (Miller et al., 1991). The anti-Ca^{2+} pump antibody that we have used, monoclonal antibody IID8, reacts with both the SERCA 2A and 2B isoforms (Plessers et al., 1991), but it may not recognize other minor isoforms of the Ca^{2+} pump. The gross distribution of Ca^{2+} pump immunoreactivity closely resembles the previous localization of Ca^{2+} pump mRNA by *in situ* hybridization and Ca^{2+} uptake in brain sections (Miller et al., 1991; Verma et al., 1992). Other minor Ca^{2+} pump isoforms may be localized to the regions where discrepancies between Ca^{2+} release channels and Ca^{2+} pumps were noted. Alternatively, our antibodies against the IP_3R might recognize inactive IP_3R or a plasma membrane form of the receptor in the areas mentioned such as that identified in olfactory neurons (Ronnett and Snyder, 1992; Cunningham et al., 1993) and T-lymphocytes (Kuno and Gardner, 1987; Khan et al., 1992) and suggested in liver (Guillemette et al., 1988; Rossier et al., 1991; Sharp et al., 1992) and pancreas (Sharp et al., 1992). A plasma membrane form of the IP_3R would not be expected to be associated with intracellular Ca^{2+} pumps.

Recently, a number of new isoforms of the IP_3R have been identified by molecular cloning techniques and shown by use of the PCR to be present in the brain (Sudhof et al., 1991; Ross et al., 1992). These isoforms are apparently of much lower abundance than the form originally identified (Sudhof et al., 1991; Ross et al., 1992). Two genes for the RyR were originally identified as the skeletal muscle and cardiac RyR genes (Takeshima et al., 1989; Nakai et al., 1990; K. Otsu et al., 1990; Zorazto et al., 1990). Northern blot analysis revealed the presence of cardiac-like RyR mRNA in the brain (Nakai et al., 1990). Recently, a new gene encoding an RyR-like protein has been cloned (Giannini et al., 1992; Hakamata et al., 1992). Northern blot analysis showed that mRNA encoded by the new gene is present in the brain, especially in the corpus striatum, thalamus, and hippocampus but is undetectable in cerebellum and cerebral cortex, while the cardiac-like RyR mRNA has a more even distribution in the brain (Hakamata et al., 1992). The relative abundance of the two gene products in the brain has not been determined. Since we detect RyR in all these brain regions and the relative intensity of staining of various regions corresponds closely to relative levels of RyR detected in membranes of the same regions by radioligand binding techniques (not shown), it is unlikely that a major isoform of the RyR has gone undetected in our present work. In addition, our results are generally consistent with a recent autoradiographic study (Padua et al., 1992). Similar arguments hold for the IP_3R in the brain (Worley et al., 1986; Sharp et al., 1993).

In conclusion, our results, along with those of others, suggest similarly important roles for caffeine- and IP_3-sensitive Ca^{2+} pools in the regulation of neuronal intracellular Ca^{2+}. The distinct localization of the IP_3R and RyR at both regional and subcellular levels suggests that the roles of the two pools in controlling intracellular Ca^{2+} in neurons are largely distinct. However, the coexistence of the two receptors in the same parts of some cells suggests that, in some instances, the two pools might interact in different ways depending on the predominance of a given release mechanism and how closely the two release channels are located.

References

Allbritton NL, Meyer T, Stryer L (1992) Range of messenger action of calcium ion and inositol 1,4,5-trisphosphate. Science 258:1812–1815.

Anderson K, Lai FA, Liu Q-Y, Rousseau E, Erickson HP, Meisser G (1989) Structural and functional characterization of the purified cardiac ryanodine receptor-Ca^{2+} release channel complex. J Biol Chem 264:1329–1335.

Berridge MJ (1990) Calcium oscillations. J Biol Chem 265:9583–9586.

Berridge MJ, Galione A (1988) Cytosolic calcium oscillations. FASEB J 2:3074–3082.

Burgoyne RD, Cheek TR (1991) Locating intracellular calcium stores. Trends Biol Sci 16:319–320.

Burk SE, Lytton J, MacLennan DH, Hull GE (1989) cDNA cloning, functional expression, and mRNA tissue distribution of a third organellar Ca^{2+} pump. J Biol Chem 264:18561–18568.

Chan JC, Aoki VM, Pickel VM (1990) Optimization of differential immunogold-silver and peroxidase labeling with maintenance of ultrastructure in brain sections before plastic embedding. J Neurosci Methods 33:113–127.

Cunningham AM, Ryugo DK, Sharp AH, Reed RR, Ronnett GV, Snyder SH (1993) Neuronal inositol 1,4,5-trisphosphate receptor localized to the plasma membrane of olfactory cilia. Neuroscience, in press.

Ehrlich BE, Watras J (1988) Inositol 1,4,5-trisphosphate activates a channel from smooth muscle sarcoplasmic reticulum. Nature 336: 583–586.

Ellisman MH, Deerinck TJ, Ouyang Y, Beck CF, Tanksley SJ, Walton PD, Airey JA, Sutko JL (1990) Identification and localization of ryanodine binding proteins in the avian central nervous system. Neuron 5:135–146.

Endo M (1977) Calcium release from the sarcoplasmic reticulum. Physiol Rev 57:71–108.

Fabiato A (1983) Calcium-induced release of calcium from the cardiac sarcoplasmic reticulum. Cell Physiol 245:C1–C14.

Fleischer S, Inui M (1989) Biochemistry and biophysics of excitation-contraction coupling. Annu Rev Biophys Biophys Chem 18:333–364.

Friel DD, Tsien RW (1992a) Phase-dependent contributions from Ca^{2+} entry and Ca^{2+} release to caffeine-induced $[Ca^{2+}]_i$ oscillations in bullfrog sympathetic neurons. Neuron 8:1109–1125.

Friel DD, Tsien RW (1992b) $[Ca^{2+}]_i$: relaxations and oscillations following changes in voltage-dependent Ca^{2+} entry and Ca^{2+}-induced Ca^{2+} release in bullfrog sympathetic neurons. Soc Neurosci Abstr 18: 972.

Furuichi T, Yoshikawa S, Miyawaki A, Wada K, Maeda N, Mikoshiba K (1989) Primary structure and functional expression of the inositol 1,4,5-trisphosphate-binding protein P400. Nature 342:32–38.

Giannini G, Clementi E, Ceci R, Marziali G, Sorrentino V (1992) Expression of a ryanodine receptor-Ca^{2+} channel that is regulated by TGF-beta. Science 257:91–94.

Giloh H, Sedat JW (1982) Fluorescence microscopy: reduced photobleaching of rhodamine and fluorescein protein conjugates by *n*-propyl gallate. Science 217:1252–1255.

Glaum SR, Scholz WK, Miller RJ (1990) Acute- and long-term glutamate-mediated regulation of $[Ca^{++}]_i$ in rat hippocampal pyramidal neurons *in vitro*. J Pharmacol Exp Ther 253:1293–1302.

Goldbeter A, Dupont G, Berridge MJ (1990) Minimal model for signal-induced Ca^{2+} oscillations and for their frequency in coding through protein phosphorylation. Proc Natl Acad Sci USA 87:1461–1465.

Guillemette G, Balla T, Baukal AJ, Catt KJ (1988) Characterization of inositol 1,4,5-trisphosphate receptors and calcium mobilization in a hepatic plasma membrane fraction. J Biol Chem 263:4541–4548.

Guthrie PB, Segal M, Kater SB (1991) Independent regulation of calcium revealed by imaging dendritic spines. Nature 354:76–80.

Hakamata Y, Nakai J, Takeshima H, Imoto K (1992) Primary structure and distribution of a novel ryanodine receptor/calcium release channel from rabbit brain. FEBS Lett 312:229–235.

Harootunian AT, Kao JPY, Paranjape S, Tsien RY (1991) Generation

of calcium oscillations in fibroblasts by positive feedback between calcium and IP_3. Science 251:75–78.
Heimer GV, Taylor CED (1974) Improved mountant for immunofluorescence preparations. J Clin Pathol 27:254–256.
Imagawa T, Smith JS, Coronado R, Campbell KP (1987) Purified ryanodine receptor from skeletal muscle sarcoplasmic reticulum is the Ca^{2+}-permeable pore of the calcium release channel. J Biol Chem 262:16636–16643.
Inui M, Saito A, Fleischer S (1987a) Purification of the ryanodine receptor and identity with feet structures of junctional terminal cisternae of sarcoplasmic reticulum from fast skeletal muscle. J Biol Chem 262:1740–1747.
Inui M, Saito A, Fleischer S (1987b) Isolation of the ryanodine receptor from cardiac sarcoplasmic reticulum and identity with the feet structures. J Biol Chem 262:15637–15642.
Irving AJ, Collingridge GL, Schofield JG (1992) Interactions between Ca^{2+} mobilizing mechanisms in cultured rat cerebellar granule cells. J Physiol (Lond) 456:667–680.
Jorgenson AO, Arnold W, Pepper DR, Kahl SD, Mandel F, Campbell KP (1988) A monoclonal antibody to the Ca^{2+}-ATPase of cardiac sarcoplasmic reticulum cross-reacts with slow type 1 but not with fast type 2 canine skeletal muscle fibers: an immunocytochemical and immunochemical study. Cell Motil Cytoskel 9:164–174.
Khan AA, Steiner JP, Snyder SH (1992) Plasma membrane inositol 1,4,5-trisphosphate receptor of lymphocytes: selective enrichment in sialic acid and unique binding specificity. Proc Natl Acad Sci USA 89:2849–2853.
King JC, Lechan RM, Kugel G, Anthony ELP (1983) Acrolein: a fixative for immunocytochemical localization of peptides in the central nervous system. J Histochem Cytochem 31:62–68.
Kuno M, Gardner P (1987) Ion channels activated by inositol 1,4,5-trisphosphate in plasma membrane of human T-lymphocytes. Nature 326:301–304.
Laemmli UK (1970) Cleavage of structural proteins during the assembly of the head of bacteriophage T4. Nature 227:680–685.
Masurovsky ER, Bunge RP (1968) Fluoroplastic coverslips for long-term nerve tissue culture. Stain Technol 43:161–165.
McPherson PS, Campbell KP (1990) Solubilization and biochemical characterization of the high affinity [^{3}H]ryanodine receptor from rabbit brain membranes. J Biol Chem 265:18454–18460.
McPherson PS, Kim YK, Valdivia H, Knudson MC, Takekura H, Franzini-Armstrong C, Coronado R, Campbell KP (1991) The brain ryanodine receptor: a caffeine-sensitive calcium release channel. Neuron 7:17–25.
Meyer T (1991) Cell signalling by second messenger waves. Cell 64: 675–678.
Mignery GA, Sudhof TC, Takei K, DeCamilli P (1989) Putative receptor for inositol 1,4,5-trisphosphate similar to ryanodine receptor. Nature 342:192–195.
Mignery GA, Newton CL, Archer BT III, Sudhof TC (1990) Structure and expression of the rat inositol 1,4,5-trisphosphate receptor. J Biol Chem 265:12679–12685.
Miller KK, Verma A, Snyder SH, Ross CA (1991) Localization of an endoplasmic reticulum calcium ATPase mRNA in rat brain by *in situ* hybridization. Neuroscience 43:1–9.
Miller RJ (1992) Neuronal Ca2+: getting it up and keeping it up. Trends Neurosci 15:317–319.
Miyazaki S-I, Yuzaki M, Nakada K, Shirakawa H, Nakanishi S, Nakade S, Mikoshiba K (1992) Block of Ca^{2+} wave and Ca^{2+} oscillation by antibody to the inositol 1,4,5-trisphosphate receptor in fertilized hamster eggs. Science 257:251–255.
Muller W, Connor JA (1991) Dendritic spines as individual neuronal compartments of synaptic Ca^{2+} responses. Nature 354:73–76.
Murphy SN, Miller RJ (1989) Two distinct quisqualate receptors regulate Ca^{2+} homeostasis in hippocampal neurons *in vitro*. Mol Pharmacol 35:671–680.
Nabauer M, Callewaert G, Cleemann L, Morad M (1989) Regulation of calcium release is gated by calcium current, not gating charge, in cardiac myocytes. Science 244:800–803.
Nakai J, Imagawa T, Hakamat Y, Shigekawa M, Takeshima H, Numa S (1990) Primary structure and functional expression from cDNA of the cardiac ryanodine receptor/calcium release channel. FEBS Lett 271:169–177.
Nakanishi S, Maeda N, Mikoshiba K (1991) Immunohistochemical localization of an inositol 1,4,5-trisphosphate receptor, P400, in neural tissue: studies in developing and adult mouse brain. J Neurosci 11:2075–2086.
Otsu H, Yamamoto A, Maeda N, Mikoshiba K, Tashiro Y (1990) Immunogold localization of inositol 1,4,5-trisphosphate (InsP3) receptor in mouse cerebellar Purkinje cells using three monoclonal antibodies. Cell Struct Funct 15:163–173.
Otsu K, Willard HF, Khanna VK, Zorzato F, Green MN, MacLennan DH (1990) Molecular cloning of cDNA encoding the Ca^{2+} release channel (ryanodine receptor) of rabbit cardiac muscle sarcoplasmic reticulum. J Biol Chem 265:13472–13483.
Padua RA, Wan W, Nagy JI, Geiger JD (1991) [^{3}H]ryanodine binding sites in rat brain demonstrated by membrane binding and autoradiography. Brain Res 542:135–140.
Padua RA, Yamamoto T, Fyda D, Sawchuk MA, Geiger JD, Nagy JI (1992) Autoradiographic analysis of [^{3}H]ryanodine binding sites in rat brain: regional distribution and the effects of lesions on sites in the hippocampus. J Chem Neuroanat 5:63–73.
Palade P, Dettbarn C, Alderson B, Volpe P (1987) Pharmacologic differentiation between inositol-1,4,5-trisphosphate-induced Ca^{2+} release and Ca^{2+}- or caffeine-induced Ca^{2+} release from intracellular membrane systems. Mol Pharmacol 36:673–680.
Parys JB, Sernett SW, DeLisle S, Snyder PM, Welsh MJ, Campbell KP (1992) Isolation, characterization, and localization of the inositol 1,4,5-trisphosphate receptor protein in *Xenopus laevis* oocytes. J Biol Chem 267:18776–18782.
Plessers L, Eggermont JA, Wuytack F, Casteels R (1991) A study of the organellar Ca^{2+}-transport ATPase isozymes in pig cerebellar Purkinje neurons. J Neurosci 11:650–656.
Randriamampita C, Bismuth G, Trautmann A (1991) Ca^{2+} induced Ca^{2+} release amplifies the Ca^{2+} response elicited by inositol trisphosphate in macrophages. Cell Regul 2:513–522.
Ronnett GV, Snyder SH (1992) Molecular messengers of olfaction. Trends Neurosci 15:508–513.
Ross CA, Meldolesi J, Milner TA, Satoh T, Supattapone S, Snyder SH (1989) Inositol 1,4,5-trisphosphate receptor localized to endoplasmic reticulum in cerebellar Purkinje neurons. Nature 339:468–470.
Ross CA, Danoff SK, Schell MJ, Snyder SH, Ullrich A (1992) Three additional inositol 1,4,5-trisphosphate receptors: molecular cloning and differential localization in brain and peripheral tissues. Proc Natl Acad Sci USA 89:4265–4269.
Rossier MF, Bird GSJ, Putney JW Jr (1991) Subcellular distribution of the calcium-storing inositol 1,4,5-trisphosphate-sensitive organelle in rat liver. Biochem J 274:643–650.
Satoh T, Ross CA, Villa A, Supattapone S, Pozzan T, Snyder SH, Meldolesi J (1990) The inositol 1,4,5-trisphosphate receptor in cerebellar Purkinje cells: quantitative immunogold labeling reveals concentration in an ER subcompartment. J Cell Biol 111:615–624.
Sharp AH, Snyder SH, Nigam SK (1992) Inositol 1,4,5-trisphosphate receptors: intracellular localization in pancreas. J Biol Chem 267: 7444–7449.
Sharp AH, Dawson TM, Ross CA, Fotuhi M, Mourey RJ, Snyder SH (1993) Inositol 1,4,5-trisphosphate receptors: immunohistochemical localization of discrete areas of rat brain. Neuroscience 53:927–942.
Spencer GG, Yu X, Khan I, Grover AK (1991) Expression of isoforms of internal Ca^{2+} pump in cardiac, smooth muscle and non-muscle tissues. Biochim Biophys Acta 1063:15–20.
Sudhof TC, Newton CL, Archer BT III, Ushkaryov YA, Mignery GA (1991) Structure of a novel InsP3 receptor. EMBO J 10:3199–3206.
Supattapone S, Worley PF, Baraban JM, Snyder SH (1988) Solubilization, purification, and characterization of an inositol trisphosphate receptor. J Biol Chem 263:1530–1534.
Takei K, Stukenbrok H, Metcalf A, Mignery GA, Sudhof TC, Volpe P, De Camilli P (1992) Ca^{2+} stores in Purkinje neurons: endoplasmic reticulum subcompartments demonstrated by the heterogeneous distribution of the $InsP_3$ receptor, Ca^{2+}-ATPase, and calsequestrin. J Neurosci 12:489–505.
Takeshima H, Nishimura S, Matsumoto T, Ishida H, Kangawa K, Minamino N, Matsuo H, Ueda M, Hanaoka M, Hirose T, Numa S (1989) Primary structure and expression from complementary DNA of skeletal muscle ryanodine receptor. Nature 339:439–445.
Thayer SA, Perney TM, Miller RJ (1988) Regulation of calcium homeostasis in sensory neurons by bradykinin. J Neurosci 8:4089–4097.
Towbin H, Staehelin T, Gorden J (1979) Electrophoretic transfer of proteins from polyacrylamide gels to nitrocellulose sheets: procedure and some applications. Proc Natl Acad Sci USA 76:4350–4354.

Treves S, De Mattei M, Lanfredi M, Villa A, Green NM, MacLennan DH, Meldolesi J, Pozzan T (1990) Calreticulin is a candidate for a calsequestrin-like function in Ca^{2+}-storage compartments (calciosomes) of liver and brain. Biochem J 271:473–480.

Tsunoda Y (1991) Oscillary Ca^{2+} signalling and its cellular function. New Biol 3:3–17.

Verma A, Hirsch DJ, Snyder SH (1992) Calcium pools mobilized by calcium or inositol 1,4,5-trisphosphate are differentially localized in rat brain. Mol Biol Cell 3:621–631.

Volpe P, Alderson-Lang BH, Madeddu L, Damiani E, Collins JH, Margreth A (1990) Calsequestrin, a component of the inositol 1,4,5-trisphosphate-sensitive Ca^{2+} store of chicken cerebellum. Neuron 5:713–721.

Walton PD, Airey JA, Sutko JL, Beck CF, Mignery GA, Sudhof TC, Deerinch TJ, Ellisman MH (1991) Ryanodine and inositol trisphosphate receptors coexist in avian cerebellar Purkinje neurons. J Cell Biol 113:1145–1157.

Worley PF, Baraban JM, De Souza EB, Snyder SH (1986) Mapping second messenger systems in the brain: differential localizations of adenylate cyclase and protein kinase C. Proc Natl Acad Sci USA 83: 4053–4057.

Worley PF, Baraban JM, Snyder SH (1989) Inositol 1,4,5-trisphosphate receptor binding: autoradiographic localization in rat brain. J Neurosci 9:339–346.

Zorazto F, Fujii J, Otsu K, Phillips M, Green MN, Lai AF, Meissner G, MacLennan DH (1990) Molecular cloning of cDNA encoding human and rabbit forms of the Ca^{2+} release channel (ryanodine receptor) of skeletal muscle sarcoplasmic reticulum. J Biol Chem 265: 2244–2256.

Zupanc GKH, Airey JA, Maler L, Sutko JL, Ellisman MH (1992) Immunohistochemical localization of ryanodine binding proteins in the central nervous system of gymnotiform fish. J Comp Neurol 325: 135–151.